JOURNAL OF VIROLOGY, Sept. 1989, p. 3884–3893
0022-538X/89/093884-10$02.00/0

Vol. 63, No. 9

Leader-Encoded Open Reading Frames Modulate Both the Absolute and Relative Rates of Synthesis of the Virion Proteins of Simian Virus 40

SYLVIA A. SEDMAN,† PETER J. GOOD,‡ AND JANET E. MERTZ*

McArdle Laboratory for Cancer Research, University of Wisconsin, Madison, Wisconsin 53706

Received 6 February 1989/Accepted 24 May 1989

Numerous viral and cellular RNAs are polycistronic, including several of the late mRNA species encoded by simian virus 40 (SV40). The functionally bicistronic major late 16S and functionally tricistronic major late 19S mRNA species of SV40 contain the leader-encoded open reading frames (ORFs) LP1, located upstream of the sequence encoding the virion protein VP1, and LP1*, located upstream of the sequence encoding the virion proteins VP2 and VP3. To determine how these leader ORFs affect synthesis of the virion proteins, monkey cells were transfected with viral mutants in which either the leader-encoded translation initiation signal was mutated or the length and overlap of the leader ORF relative to the ORFs encoding the virion proteins were altered. The levels of initiation at and leaky scanning past each initiation signal were determined directly by quantitative analysis of the viral proteins synthesized in cells transfected with these mutants. Novel findings from these experiments included the following. (i) At least one-third of ribosomes bypass the leader-encoded translation initiation signal, GCCAUGG, on the SV40 major late 16S mRNA. (ii) At least 20% of ribosomes bypass even the consensus translation initiation signal, ACCAUGG, when it is situated 10 bases from the 5′ end on the major late 16S mRNA. (iii) The presence of the leader ORF on the bicistronic 16S mRNA species reduces VP1 synthesis threefold relative to synthesis from a similar RNA that lacks it. (iv) At least half and possibly all VP1 synthesized from the bicistronic 16S mRNA species is made by a leaky scanning mechanism. (v) LP1 and VP1 are synthesized from the bicistronic 16S mRNA species at approximately equal molar ratios. (vi) Approximately half of the VP1 synthesized in SV40-infected cells is synthesized from the minor, monocistronic 16S mRNA even though it accounts for only 20% of the 16S mRNA present. (vii) The presence and site of termination of translation of the leader ORF on the late 19S mRNAs affect the relative as well as absolute rates of synthesis of VP2 and VP3.

Most eucaryotic mRNAs studied to date are monocistronic, containing a single large protein-coding region beginning 20 to 100 bases from the 5′ end of the mRNA (19). However, mRNAs which contain one or more open reading frames (ORFs) upstream of the protein-coding region have also been described. Among these are a large number of viral mRNAs and mRNAs encoding the products of cellular proto-oncogenes (8, 16, 17, 19, 23, 32, and references therein). It is of interest to understand whether these ORFs affect translation of the downstream ORFs, the magnitude of the effect, and the mechanism(s) of translation of the downstream ORFs.

Translation of most eucaryotic mRNAs appears to occur by a scanning mechanism (12). According to the modified scanning model, an initiator AUG is recognized by 40S ribosomal subunits based on its location in the mRNA and the sequences surrounding it. The 40S ribosomal subunits bind at or near the 5′ end of the mRNA and scan toward the 3′ end until they encounter an AUG codon. From a survey of known translation initiation signals (13) and experiments in which the sequence surrounding an AUG codon was varied systematically (15), the optimal sequence context for efficient recognition as an initiation signal was determined to be

```
      −3      +1      +4
C  C  A  C  C  A  U  G  G
```

with the −3 and +4 positions being of primary importance. If a pyrimidine is present at the −3 or +4 position, 40S subunits frequently scan past the AUG codon and initiate downstream. Translation has also been hypothesized to occur by a reinitiation mechanism in which ribosomes that have translated one ORF go on to translate a second ORF located downstream (9, 11, 21, 26, 30). Lastly, downstream ORFs on some mRNAs (e.g., picornavirus mRNAs) are translated in eucaryotic cells by direct internal initiation (10, 27).

Several of the simian virus 40 (SV40) late mRNA species are functionally polycistronic, containing two to four protein-coding regions (Fig. 1). These viral late mRNAs encode the virion proteins VP1, VP2, and VP3 and the leader-encoded proteins LP1 (also called agnoprotein) and LP1*. The two size classes of late mRNAs, 16S and 19S, are defined by the 3′ splice site used in processing the primary transcript (Fig. 1). All of the 16S mRNAs encode VP1; the most abundant (i.e., the major 16S mRNA species [E in Fig. 1]) encodes LP1 as well (1). Each of the 19S mRNA species encode all three virion proteins; however, only VP2 and VP3 are synthesized from these mRNAs (5). Most, if not all, of VP3 synthesis from the 19S mRNAs of SV40 occurs by leaky scanning past the weak VP2 translation initiation signal (UCCAUGG) (2, 30). The major 19S mRNA species (B in Fig. 1) contains a small leader-encoded ORF that encodes LP1*, a 30-amino-acid polypeptide that begins with the same translation initiation signal as the LP1 ORF. Because this

* Corresponding author.
† Present address: Laboratory of Cellular Oncology, National Cancer Institute, Bethesda, MD 20892.
‡ Present address: Laboratory of Molecular Genetics, National Institute of Child Health and Human Development, Bethesda, MD 20892.

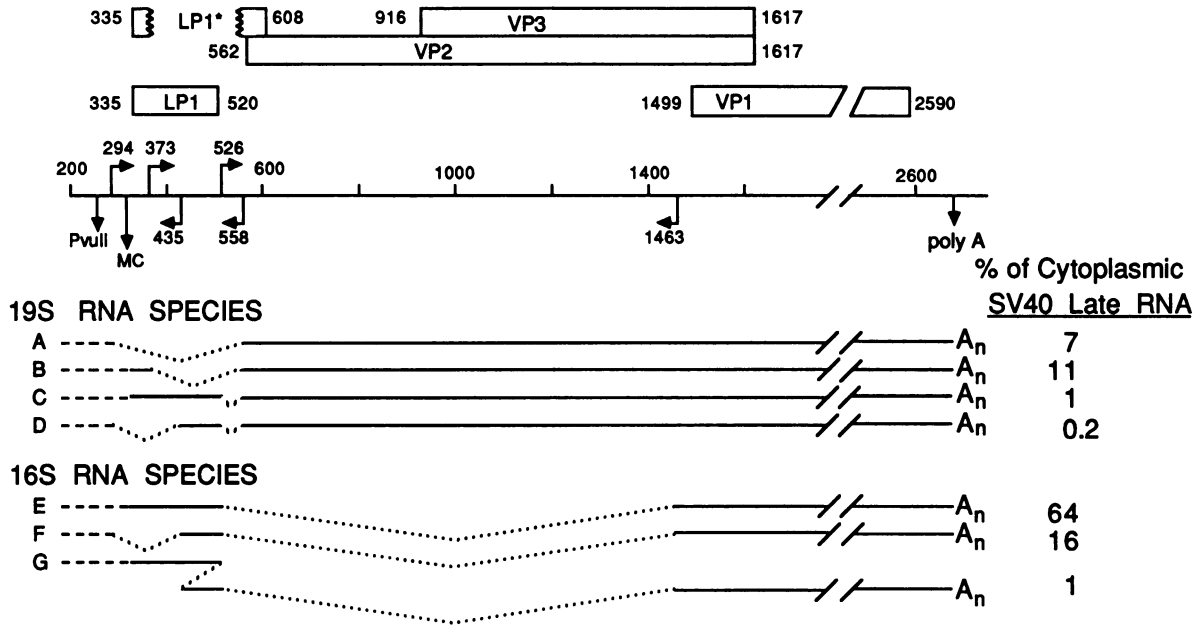

FIG. 1. Map of the late region of SV40. The numbered line represents SV40 DNA with the nucleotide residues given in the SV numbering system (31). The structures of the 19S and 16S mRNA species are shown, with the locations of the excised sequences (.....) indicated. The 5′ ends (- - - - -) of these RNAs are heterogeneous, with the major cap site (MC) mapping to nt 325. The arrows pointing to the right and left indicate the locations of 5′ and 3′ splice sites, respectively. The relative amounts of each spliced species found in the cytoplasm of infected cells as determined by Good et al. (6) are listed at the right. Species G contains a tandem duplication of nt 435 through 526. The proteins encoded by these RNAs are indicated by the boxes labeled LP1, VP2, VP3, and VP1; the numbers adjacent to the boxes indicate the first and last nucleotide residues translated. LP1*, an ORF present on 19S mRNA species B, is also shown; the discontinuity in the ORF relative to the DNA sequence ( ), due to removal of an intron, is indicated.

initiation signal lies upstream of the sequences encoding the virion proteins on the majority of mRNAs used to synthesize these proteins, we wanted to know whether the LP1 initiation signal affects translation of the ORFs located downstream and the mechanism of synthesis of the virion proteins from these messages.

To study the translation of specific SV40 late mRNAs, we constructed splice site mutants that, when transfected into monkey cells, synthesize only the major 16S or major 19S mRNA species. To determine how the leader ORFs affect synthesis of the virion proteins from the major late mRNAs, derivatives of these mutants were constructed in which either the LP1 initiation signal was mutated or the site of termination of translation of the leader ORF was altered. Quantitative analysis of the viral proteins synthesized in cells transfected with these mutants indicated that the presence of the leader ORFs both decreases synthesis of the virion proteins from the major mRNA species and affects the rate of synthesis of VP2 relative to that of VP3. In addition, at least half of VP1 is synthesized from the bicistronic 16S mRNA species by a leaky scanning mechanism.

MATERIALS AND METHODS

Cell lines and culture conditions. BSC-1 cells, an African green monkey kidney cell line, were used in all transfection experiments. MA-134 cells were used to grow virus stocks, and CV-1P cells were used to determine the titers of the virus stocks. The cells were maintained and infected with virus (30 to 40 PFU/cell) essentially as described by Mertz and Berg (24). Transfections were performed as described previously (30).

Antisera. Polyclonal antisera raised against gel-purified VP1 and VP3 were described previously (30).

Construction of mutants. The nomenclature used is as follows: a p preceding a mutant name indicates that the DNA is in plasmid form; a mutant name without p refers to the corresponding DNA in which the vector sequences have been removed by digestion with *Eco*RI. Mutants have been named according to the RNA being studied (major 16S or major 19S) followed by the distance between the site of termination of the leader ORF and the most upstream virion protein initiation signal. For example, SV16S(−21) refers to a mutant that when transfected into monkey cells produces only the major 16S mRNA, with the LP1 ORF terminating 21 bases upstream of the VP1 initiation signal.

pSVS is the complete viral genome of SV40 strain WT830 cloned at the *Eco*RI site into a pBR322-based plasmid (4). The plasmid pSV1768(*dpm*435) is a derivative of pSVS and contains two point mutations in the late leader region that inactivate the 3′ splice site at nucleotide (nt) 435 and alter a single amino acid in LP1 (6). Plasmid pSV16S(−21), the parent plasmid for the construction of the 16S series mutants, was made from pSV1768(*dpm*435) by the deletion of 30 base pairs from nt 1464 through 1493 (inclusive), with the insertion of GGTCGA at the site of the deletion. Plasmid pSV16S(+115) was made from pSV16S(−21) by deletion of the small *Hpa*I fragment from nt 502 through 521, inclusive. This 20-base-pair fragment includes the translation termination codon of the LP1 ORF. Mutant pSV16S(fusion) was constructed from pSV16S(−21) by removal of the 20-base-pair fragment from nt 502 through 521 and insertion of an 8-base-pair *Sal*I linker (GGTCGACC) at that site. Mutant pSV*pm*1493 contains a point mutation at nt 335 which changes the LP1 translation initiation codon to UUG (29). Plasmid pSV16S(LP1 AUG$^-$), a derivative of SV16S(−21) lacking the LP1 translation initiation signal, was made by

recombination of the larger *Nae*I (SV40 nt 345)-to-*Bst*XI (SV40 nt 4759) fragment of pSV16S(−21) with the smaller *Bst*XI-to-*Nae*I fragment of the mutant pSV*pm*1493. Plasmid pSV16S (ACCAUGG), a derivative of pSV16S(−21) containing a point mutation that changes the LP1 translation initiation signal from GCCAUGG to ACCAUGG, was constructed by site-directed mutagenesis of pSV16S(−21) using the Mutagene in vitro mutagenesis kit (Bio-Rad Laboratories) essentially as described in the instruction manual. Plasmid pSV16S(fusion-ACCAUGG) was constructed by recombination of the smaller *Kpn*I (SV40 nt 294)-to-*Nae*I (SV40 nt 346) fragment of pSV16S(ACCAUGG) with the larger *Kpn*I-to-*Nae*I fragment of pSV16S(fusion).

pSV19S(+48) (previously called pSV1770) (5), the parent plasmid for the construction of the 19S series mutants, contains a substitution of CCTCGAGG in place of nt 294 through 298, inclusive; this mutation results in the inactivation of the 5′ splice site at nt 294. pS+8 is a mutant in which the sequence GGTCGACCCG has been inserted between nt 348 and 349 (4), resulting in a frameshift mutation in the LP1 ORF. pSV19S(−5) was made from pS+8 by substitution of the sequence CCTCGAGG in place of nt 295 through 298, inclusive. pSV19S(fusion) was made from pSV19S(+48) by insertion of GGTCGACC between nt 348 and 349. pSV19S(LP1 AUG$^-$) is a double mutant containing both a substitution of CTCTAGAG in place of nt 295 through 298 and the LP1 AUG point mutation. The structures of all mutants were confirmed by DNA sequence analysis.

Analysis of virion proteins. VP1-related proteins synthesized in cells transfected with the 16S mRNA series mutants were analyzed by immunoprecipitation with antiserum raised against VP1, followed by treatment with cells of *Staphylococcus aureus*. Forty hours posttransfection, cells were preincubated in medium lacking methionine for 1 h; this was followed by the addition of [^{35}S]methionine (50 μCi/ml, >1,000 Ci/mmol) and incubation for 30 min at 37°C. Protein was extracted as described previously (30). VP1-related proteins were immunoprecipitated and analyzed by electrophoresis in a 12% polyacrylamide (0.35% bis-acrylamide) gel containing sodium dodecyl sulfate (SDS). The gel was impregnated with En^{3}Hance (Du Pont, NEN Research Products), dried, and exposed to X-ray film. The relative amounts of radioactivity in the protein bands were determined by laser densitometry. The ratio of two VP1-related proteins synthesized from a single mRNA species was determined directly by quantitative densitometric analysis of the bands within a single lane of an autoradiogram (e.g., see Fig. 3B, lane 3, and Fig. 7). Multiple exposures were taken of each gel to insure that the response was in the linear range of the film. In addition, serial dilutions were included on each gel. When comparisons were made between samples, the relative amount of radioactivity in each protein band was normalized to the relative amount of cytoplasmic viral late 16S mRNA present in cells transfected in parallel to correct for possible differences in mRNA levels caused by differences in transfection efficiencies or half-lives of the various mutant mRNAs. mRNA levels rarely varied within an experiment by more than 50% (e.g., see Fig. 3C).

VP3-related proteins synthesized in cells transfected with the 19S series mutants were also analyzed by immunoprecipitation. Experiments were done essentially as described for the 16S series mutants except that the cells were incubated in medium lacking arginine for 2 h before being labeled and then were incubated in arginine-free medium containing [^{14}C]arginine (10 μCi/ml, 325 mCi/mmol) for 1 h. Immunoprecipitation procedures were performed by using antiserum raised against VP3.

To measure directly the rate of synthesis of LP1 relative to that of VP1 from each 16S mRNA species, cells were infected with virus stocks of the mutants indicated at a multiplicity of infection of 30 to 40 PFU per cell. At 48 h postinfection, the cells were labeled with [^{14}C]arginine and harvested as described above. Analysis of the labeled proteins was accomplished by loading equal counts per minute of each sample onto 12% polyacrylamide gels (0.35% bis-acrylamide) containing SDS. The amount of LP1 relative to that of VP1 in each sample was determined by laser densitometry, with appropriate corrections being made for differences in arginine incorporation (LP1 and VP1 contain 8 and 13 arginine residues per molecule, respectively) and the 1-h half-life of the LP1 encoded by SV16S(−21) (data not shown).

Analysis of viral late mRNAs. Cytoplasmic RNA samples were purified from mutant-transfected cells, and S1 nuclease-mapping analysis was used to quantify the amount of SV40 late 16S or 19S RNA present in each sample essentially as described previously (30). Viral late 16S or 19S mRNA and cellular β-actin mRNA were quantified simultaneously; the latter served as an internal control to correct for variations in RNA recoveries during purification and S1 nuclease mapping (30).

To determine the distribution of the 5′ ends of the viral late mRNAs, primers spanning SV40 nt 1543 through 1526 and nt 604 through 585 were used for analysis of viral late 16S and 19S mRNAs, respectively. The distributions of the 5′ ends of the RNAs made from the 16S series mutants were not affected by the mutations introduced into the SV40 genome. For the 19S series mutants, the distributions of the 5′ ends were affected by the substitution mutations at the *Kpn*I (nt 294) site, but the changes were similar for all mutants (data not shown). To determine which of the intervening sequences were excised in synthesis of the viral mRNAs made in cells transfected with each mutant, a modified primer extension technique was performed in which an oligonucleotide spanning nt 261 through 279 was annealed to the cDNAs and the cDNAs were cleaved with *Pvu*II to generate a single 3′ end as described previously (6).

RESULTS

Experimental design. The major late 16S mRNA species (E in Fig. 1) is functionally bicistronic, encoding both VP1, the major protein component of the virion particle, and LP1, a 61-amino-acid leader-encoded protein. Since the LP1 ORF lies upstream of the sequences encoding VP1, we wanted to determine how it affects VP1 synthesis from this mRNA. SV40-infected monkey cells also synthesize two minor late 16S mRNA species (species F and G in Fig. 1), one of which lacks the LP1 AUG. To study the mechanism of synthesis of VP1 from the major 16S mRNA species, we constructed pseudo-wild-type (WT) SV16S(−21), which, when transfected into monkey cells, results in the synthesis of only the major bicistronic mRNA species because the 3′ splice site at nt 435 which is needed for synthesis of the two minor 16S mRNA species has been inactivated (6) (Fig. 2). In addition, the translation termination codons present in the intercistronic sequences between the LP1 and VP1 ORFs on WT 16S mRNA have been deleted in this mutant, so that subsequent removal of the LP1 termination codon results in translation from the leader region proceeding into the VP1 ORF (see below). Although the 19S RNA species are pro-

duced in cells transfected with SV16S(−21), VP1 is not synthesized from these RNAs (5).

Effect of LP1 ORF on VP1 synthesis. To determine whether the presence of the LP1 ORF affects synthesis of VP1 from the major 16S mRNA, monkey cells were transfected in parallel with SV16S(−21) and SV16S(LP1 AUG⁻). Mutant SV16S(LP1 AUG⁻) differs from SV16S(−21) by a single-base-pair change which results in the inactivation of the LP1 initiation signal, thereby making the 16S mRNA synthesized from it monocistronic (Fig. 3A). At 40 h posttransfection, the cells were labeled for 30 min with [^{35}S]methionine and harvested immediately thereafter. The relative amounts of radiolabeled VP1 present in cells were determined by immunoprecipitation with antiserum to VP1 followed by polyacrylamide gel electrophoresis, autoradiography, and densitometric analysis of the resulting autoradiograms (Fig. 3B). To determine the relative rates of synthesis of VP1 synthesized from the mutants, the relative amounts of radiolabeled VP1 were normalized to the relative amounts of cytoplasmic SV40 late 16S mRNA present in cells transfected in parallel with the same DNAs (Fig. 3C). Cytoplasmic viral 16S mRNA was normalized to cellular β-actin mRNA to control for RNA recovery. Cells transfected with SV16S(LP1 AUG⁻) DNA reproducibly synthesized threefold more VP1 than cells transfected with the pseudo-WT 16S(−21) (Fig. 3A). Therefore, the presence of the LP1 ORF significantly decreases synthesis of VP1 from the major 16S mRNA species.

Ribosomes bypass the LP1 initiation signal at a high frequency. The LP1 initiation signal is present in a strong sequence context (i.e., GCCAUGG). To measure directly the percentage of ribosomes that bypass the LP1 initiation signal and initiate downstream at VP1, the mutant SV16S(fusion), which lacks the LP1 termination codon such that the LP1 ORF is fused to the VP1 ORF (Fig. 3A), was constructed. VP1 synthesis in cells transfected with this mutant should be due solely to scanning because ribosomes initiating at the LP1 AUG can synthesize only an LP1-VP1 fusion protein. The efficiency of translation initiation at the LP1 relative to that at the VP1 initiation signal can be determined directly by a pulse-labeling experiment without normalization to viral mRNA levels, since both VP1 and the fusion protein are synthesized from the same mRNA and can be immunoprecipitated with the same polyclonal antiserum raised against VP1. Although the LP1 sequences present on the amino terminus of the fusion protein may mask some VP1 epitopes, the use of a polyclonal serum should yield quantitative immunoprecipitation of the fusion protein as well as VP1.

Monkey cells were transfected in parallel with SV16S (fusion) and SV16S(−21) DNA and labeled with [^{35}S]methionine, and VP1-related proteins were immunoprecipitated and analyzed by polyacrylamide gel electrophoresis. As expected, cells transfected with SV16S(fusion) synthesized both the LP1-VP1 fusion protein and VP1 (Fig. 3B). Quantitation of the relative amounts of radioactivity in the two bands indicated that the rate of synthesis of the fusion protein relative to that of VP1 was 1:0.5. In other words, one-third of the 40S ribosomal subunits bypassed the LP1 initiation signal and initiated at the VP1 initiation signal.

Also noteworthy is the finding that VP1 was synthesized at a rate in cells transfected with SV16S(fusion) half that in cells transfected with SV16S(−21) (Fig. 3). Therefore, at least half of VP1 synthesized from the bicistronic 16S mRNA is made via a leaky scanning mechanism.

Reduction in VP1 synthesis when the LP1 ORF terminates 115 bases beyond the VP1 initiation signal. To determine whether the location of the termination codon of the LP1 ORF affects synthesis of VP1, SV16S(+115), a third variant of SV16S(−21) which lacks nt 502 through 521, was constructed. In cells transfected with this mutant, ribosomes initiating at the LP1 initiation signal do not encounter a translation termination signal until 115 bases beyond the VP1 initiation codon (Fig. 3A). Cells transfected with this mutant synthesized VP1 at rates similar to that seen in cells transfected with SV16S(fusion) (Fig. 3).

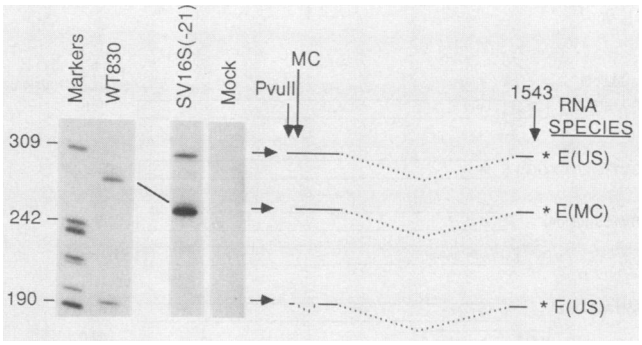

FIG. 2. Qualitative analysis by a modification of the primer extension technique of the SV40 late 16S mRNAs made from WT830 and pseudo-WT SV16S(−21). cDNAs of cytoplasmic RNA purified from 10^4 BSC-1 cells infected with virus made from WT830 and SV16S(−21) were synthesized by hybridization of a synthetic oligonucleotide 5′ end labeled at nt 1543. The primer was extended, the RNA was hydrolyzed, and an oligonucleotide spanning nt 261 through 279 (containing a *Pvu*II restriction site) was annealed to the cDNA. The samples were incubated with *Pvu*II and electrophoresed in a 5% polyacrylamide gel containing 8 M urea. The diagrams on the right indicate the structures of the cDNAs that correspond to the bands in the gel; *, locations of the radiolabeled 5′ ends. The RNAs are named as in Fig. 1. MC and US refer to RNAs with 5′ ends mapping to the major cap site and upstream of nt 273, respectively. The cDNAs made from mRNAs of 16S(−21) are smaller than those made from WT because the intercistronic distance between the LP1 and VP1 ORFs is smaller by 24 bases. Mock refers to cells that were transfected without DNA. The markers were 3′-end-labeled, *Msp*I-cut pBR322 DNA. The difference in the intensity of the signal in the lanes marked WT830 and SV16S(−21) is the result of the cells having been infected at different multiplicities of infection. Cells infected with WT SV40 do not accumulate significant quantities of RNA species E with 5′ ends mapping upstream of the *Pvu*II site at nt 272 because these transcripts are processed predominantly to RNA species F instead (P.J.G. and J.E.M., submitted for publication).

Relative rates of synthesis of LP1 and VP1 from the major 16S mRNA species. The above experiments also allow one to predict the rate of synthesis of LP1 relative to that of VP1 from the major 16S mRNA species. Since the sequence context of the leader AUG is identical in the 16S mRNAs made from SV16S(−21) and SV16S(fusion), the rate of synthesis of LP1 should be equal to the rate of synthesis of the LP1-VP1 fusion protein. From the data summarized in Fig. 3A, we know that the rate of synthesis of the LP1-VP1 fusion protein is similar to the rate of synthesis of VP1 in cells transfected with SV16S(−21). Therefore, LP1 and VP1 should be synthesized at approximately equal molar ratios from the 16S mRNA made from SV16S(−21).

To measure directly the rate of synthesis of LP1 relative to that of VP1 from the major 16S mRNA species, monkey cells were infected with SV16S(−21) virus and pulse-labeled with [^{14}C]arginine 48 h later. The proteins were separated in a 12% polyacrylamide gel containing SDS, and the relative

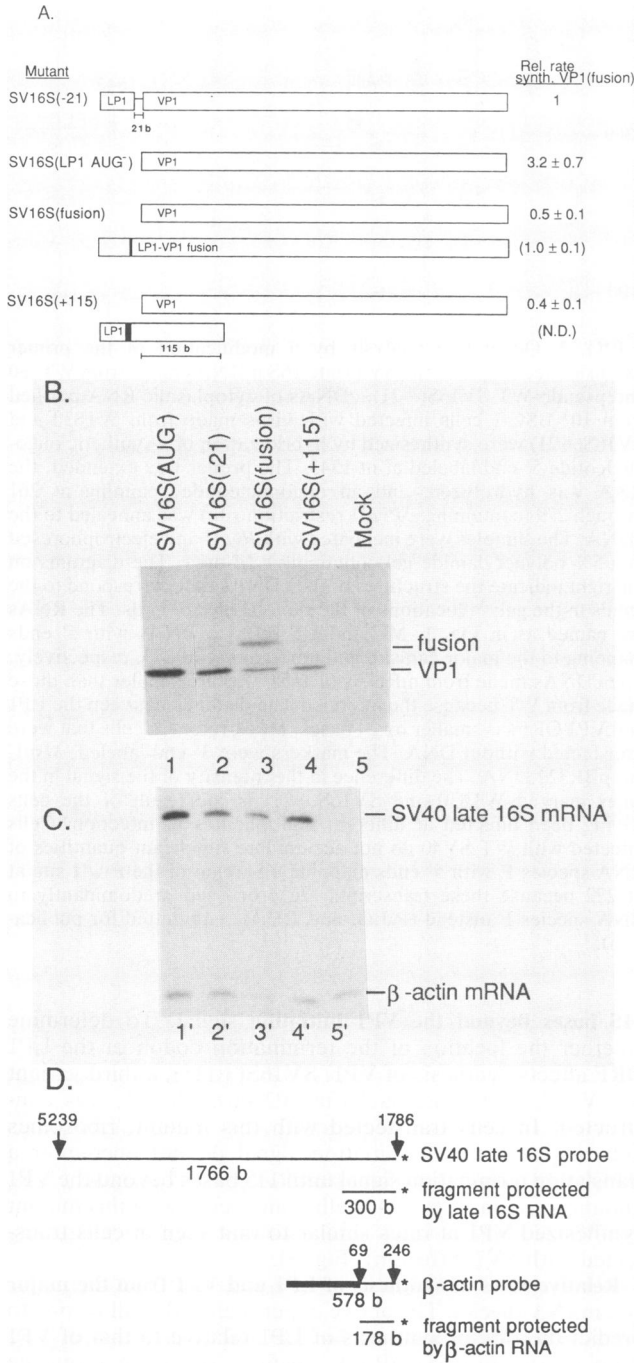

FIG. 3. Relative rates of VP1 synthesis in cells transfected with mutants in which the 16S mRNA species differ in their leader ORFs. (A) Configurations of ORFs present on the 16S mRNA synthesized and summary of data obtained from each mutant. Dark vertical lines near the carboxyl-terminal end of the LP1 ORF indicate the locations of small frameshift mutations. To the right is a summary of the rates of synthesis of VP1 and the LP1-VP1 fusion protein in cells transfected with each mutant relative to the rate of synthesis of VP1 in cells transfected in parallel with the pseudo-WT SV16S(−21). Listed are means ± standard errors of the mean of data obtained from four independent experiments similar to the one shown in panels B and C. The relative rate of synthesis of the LP1-related protein made from SV16S(+115) was not determined since it is not precipitable with VP1 antisera. b, Bases. (B) Autoradiogram of pulse-labeled, VP1-related proteins synthesized in cells transfected with the mutants indicated. At 40 h after transfection, BSC-1 cells were pulse-labeled for 30 min with [^{35}S]methionine and harvested immediately thereafter. Equal counts per minute from each lysate were immunoprecipitated with equal amounts of a polyclonal antiserum raised against VP1 and analyzed by electrophoresis through a 12% polyacrylamide gel containing SDS. Positions of the VP1 and LP1-VP1 fusion bands are indicated. The lane labeled mock contained lysate processed in parallel from cells transfected without DNA. All lanes are from a single autoradiogram; they have been reorganized to correspond with the order of presentation in the text. (C) Quantitative S1 nuclease-mapping analysis of SV40 late 16S mRNA and cellular β-actin mRNA. Cytoplasmic RNA samples harvested in parallel with the protein samples in panel B were S1 nuclease mapped simultaneously for SV40 late 16S and β-actin RNA. The ratio of these two bands in each sample was used for normalization of the relative amount of VP1 present in the corresponding sample in panel B. The positions of the bands corresponding to the viral late 16S and β-actin mRNAs are indicated. (D) Strategy used for S1 nuclease mapping. The probe used to quantify SV40 late 16S mRNA, derived from pSV16S(−21), contained SV40 nt 1786 to 5239 and was 5′-end labeled at nt 1786. Cellular β-actin mRNA was quantified by using a probe containing nt 69 through 246 of pHFβA-1 adjacent to 400 bases (b) of vector DNA (30); it was 5′ end labeled at nt 246. Thin lines, actin sequences; the thick line, sequences derived from the vector.

amounts of radiolabeled LP1 and VP1 were quantified by laser densitometry of autoradiograms (Fig. 4B). After correction for differences in arginine incorporation and the half-life of LP1, the relative rates of synthesis of the two proteins were calculated to be 1.0 ± 0.2 (Fig. 4A). Therefore, LP1 and VP1 are both synthesized fairly efficiently from this mRNA species.

Changing the distance between the LP1 and VP1 ORFs from 45 to 21 bases does not affect their relative rates of translation. Kozak (18) has suggested that reinitiation of translation occurs inefficiently when the distance between two ORFs is less than 40 to 80 bases. The intercistronic distance between the LP1 and VP1 ORFs is 21 bases for the 16S mRNA made from mutant SV16S(−21), compared with 45 bases for the major 16S mRNA made from WT SV40. If VP1 is synthesized from these bicistronic mRNAs in part by a reinitiation mechanism, the difference in the intercistronic distance between WT and pseudo-WT might differentially affect synthesis of VP1. To determine whether the distance between the LP1 and VP1 ORFs affects synthesis of VP1, the relative rates of synthesis of LP1 and VP1 were also determined in cells infected with mutant SV1768(*dpm*435). Cells infected with SV1768(*dpm*435) make only a bicistronic 16S mRNA which is essentially identical in sequence to the bicistronic 16S mRNA made from WT SV40 (6). The rate of synthesis of LP1 relative to that of VP1 in cells infected with SV1768(*dpm*435) was similar to that found in cells infected with SV16S(−21) (Fig. 4). Therefore, the difference in the intercistronic sequences present in 16S RNA made from SV16S(−21) versus WT830 does not affect the synthesis of VP1. Consequently, the results obtained with the SV16S (−21) series mutants should be applicable to WT SV40.

Approximately half of the VP1 synthesized in SV40-infected cells is made from the minor monocistronic 16S mRNA species. Cells infected with WT SV40 synthesize predominantly two species of 16S mRNA (species E and F in Fig. 1). We wanted to know how much VP1 was synthesized from each 16S mRNA species in a WT virus infection. Since LP1 is synthesized only from the bicistronic mRNA, whereas VP1 is synthesized from both 16S mRNAs, comparison of the rate of synthesis of LP1 relative to that of VP1 in monkey

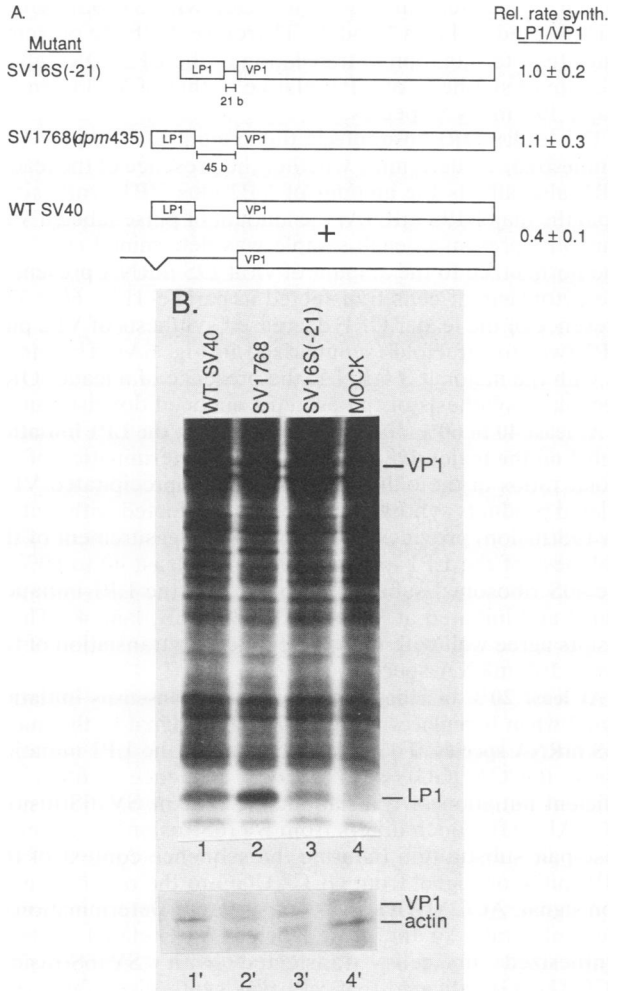

FIG. 4. Rates of synthesis of LP1 relative to that of VP1 in cells infected with WT SV40 and the mutants SV16S(−21) and SV1768. (A) Configurations of ORFs present on the 16S mRNA synthesized from each mutant. On the right is a summary of the molar rates of synthesis of LP1 relative to that of VP1 from three independent experiments similar to the one shown in panel B. Values are means ± standard errors of the mean. b, Bases. (B) Autoradiograms of pulse-labeled, VP1-related proteins synthesized in cells infected with the mutant viruses indicated. At 48 h after infection, BSC-1 cells were labeled for 1 h with [^{14}C]arginine and harvested immediately thereafter. Lysates were analyzed directly by electrophoresis in 12% polyacrylamide gels containing SDS. Bands corresponding to LP1 and VP1 are indicated. The autoradiogram at the bottom is from a gel of the same samples which was run longer to better separate VP1 from actin. The upper autoradiogram is an overexposure presented to show clearly the bands corresponding to LP1.

cells infected in parallel with WT SV40 and mutant SV1768(*dpm*435) should allow us to determine the contribution to total VP1 synthesis made by each of the 16S mRNA species. Data obtained from three independent experiments indicated that the rate of synthesis of LP1 relative to that of VP1 in cells infected with WT SV40 was one-half to one-third that seen in cells infected with SV1768(*dpm*435) (Fig. 4). Using these data, we calculated that translation of the minor 16S message accounts for approximately half of the VP1 synthesized in infected monkey cells. This finding is consistent with those presented in Fig. 3 which show that a 16S mRNA species lacking the LP1 AUG is translated

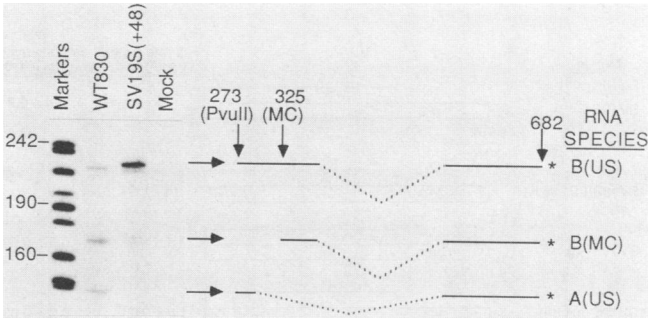

FIG. 5. Analysis by a modification of the primer extension technique of the SV40 late 19S mRNAs made from WT830 and pseudo-WT SV19S(+48). The analysis was performed as described in the legend to Fig. 2, except for the use of cytoplasmic RNA purified from 2 × 10^6 transfected BSC-1 cells and a primer 5′-end labeled at nt 682. The top band of the doublet corresponds to RNA species B; this band is larger than that seen in the WT because of the presence in the mutant RNA of 3 additional bases at nt 294. The lower band of the doublet corresponds to RNA species B with a 5′ end mapping just downstream of the *Pvu*II site.

threefold more efficiently than a bicistronic 16S mRNA. Therefore, the minor 16S mRNA species, even though it makes up only 20% of the total 16S mRNA, plays a physiologically important role in the synthesis of VP1 in cells infected with WT SV40.

The leader ORF affects the ratio of VP2 to VP3 synthesized from the major 19S mRNA species. The major 19S mRNA species contains three functional ORFs encoding VP2, VP3, and a 30-amino-acid polypeptide, which we shall call LP1* (Fig. 1). The initiation codon for this small protein is the same as that used for LP1 synthesis. Ribosomes translating the LP1* ORF terminate translation 48 bases downstream of the VP2 initiation signal.

To determine whether the presence of the LP1* ORF affects synthesis of VP2 and VP3, pseudo-WT SV19S(+48) and variants of it were constructed in which the 5′ splice site at nt 294 was inactivated. Cells transfected with such mutants synthesize primarily the major 19S mRNA species (5) (species B in Fig. 5). Monkey cells were transfected with these mutants and labeled 40 h later with [^{14}C]arginine. The amount of radiolabeled VP2 relative to that of VP3 present in each sample was determined by immunoprecipitation of both proteins by using antiserum raised against VP3. The VP2-to-VP3 ratio in cells transfected with SV19S(LP1 AUG$^-$), a variant in which the LP1 translation initiation signal had been inactivated, was twofold higher than in cells transfected with SV19S(+48) (Fig. 6B, lanes 1 and 2; summarized in Fig. 6A). Since VP2 and VP3 are synthesized concurrently from the same mRNAs (5) and were coimmunoprecipitated with VP3 antiserum, the data obtained in this experiment are subject to little error. Consequently, the twofold difference observed is real. Therefore, the presence of the LP1* ORF differentially affects the rate of synthesis of VP2 relative to that of VP3.

The variant SV19S(−5) contains a frameshift mutation located 5′ to the VP2-coding sequences such that ribosomes translating the LP1* ORF terminate 5 bases upstream of the VP2 initiation signal (Fig. 6A). Cells transfected with this mutant synthesized VP2 and VP3 at a ratio similar to that seen in cells transfected with SV19S(+48) (Fig. 6A and B, lanes 2 and 3). On the other hand, cells transfected with variant SV19S(fusion), which fuses the LP1* ORF to the VP2-VP3 ORF (Fig. 6A), synthesized VP2 and VP3 at a ratio

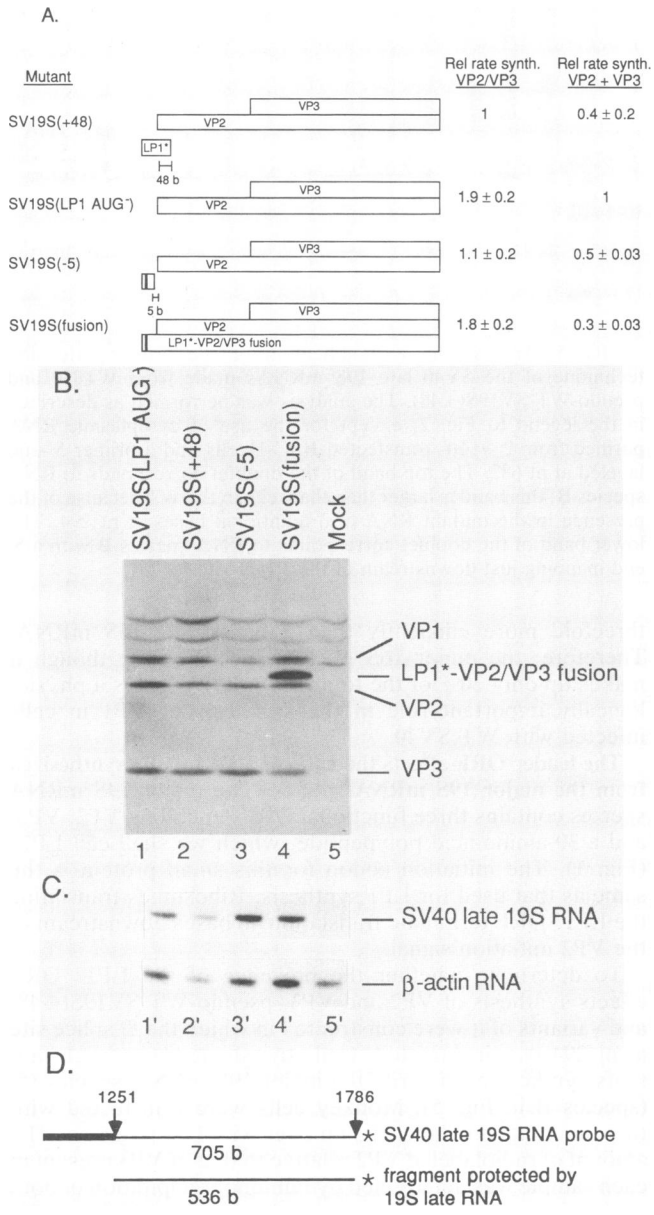

FIG. 6. Relative rates of synthesis of VP2 and VP3 in cells transfected with mutants in which the major 19S mRNA species differ in their leader ORFs. (A) Configurations of ORFs present on the 19S mRNA synthesized and summary of data obtained from each mutant. Dark vertical lines near the amino-terminal end of LP1* indicate the locations of small frameshift mutations. On the right is a summary of the rates of synthesis of VP2 relative to that of VP3 in cells transfected with each mutant normalized to the rate of synthesis of VP2 relative to that of VP3 in cells transfected with pseudo-WT SV19S(+48). These values are means ± standard errors of the mean of data obtained from two to three independent experiments similar to the one shown in panel B. Also shown are the rates of synthesis of VP2 plus VP3 in cells transfected with each mutant relative to the rate of synthesis of VP2 plus VP3 in cells transfected with S19S(LP1 AUG$^-$) (panel B), with normalization to the ratio of viral 19S mRNA to cellular β-actin found in the cytoplasm of cells transfected in parallel (panel C). b, Bases. (B) Autoradiogram of pulse-labeled, VP3-related proteins synthesized in cells transfected with the mutants indicated. At 40 h after transfection, BSC-1 cells were labeled for 1 h with [^{14}C]arginine and harvested immediately thereafter. Equal counts per minute from each lysate were immunoprecipitated with equal amounts of a polyclonal antiserum raised against VP3 and analyzed by electrophoresis through a 12% polyacrylamide gel containing SDS. The positions of the VP1, VP2, VP3, and LP1*-VP2/VP3 fusion bands are indicated at the right. VP1 coprecipitated due to aggregation with VP2 and VP3 (5). The band just below VP1, present also in the mock lane, is actin. The relative amounts of VP2 and VP3 between lanes should not be compared directly since the amount of each sample loaded on the gel was not first corrected to the relative amount of cytoplasmic SV40 late 19S mRNA present. However, since VP2 and VP3 are synthesized from the same mRNA (5), their ratios can be compared directly. (C) Quantitative S1 nuclease analysis of SV40 late 19S and β-actin mRNA. Cytoplasmic RNA samples harvested in parallel with the protein samples in panel B were S1 nuclease mapped simultaneously for SV40 late 19S and β-actin RNA. The ratio of these two bands in each sample was used for normalization of the relative amount of VP2 plus VP3 present in the corresponding sample in panel B. A single autoradiogram containing the regions of the 19S and actin bands is shown. (D) Strategy used for S1 nuclease mapping. The probe used to quantify SV40 late 19S mRNA, derived from WT SV40, contains SV40 nt 1786 to 1251 adjacent to 170 nt of vector DNA; it was 5′ end labeled at nt 1786. Thin lines, SV40 sequences; thick line, sequences derived from the vector. The β-actin probe was the same as the one used in Fig. 3. b, Bases.

similar to that seen in cells transfected with SV19S(AUG$^-$) (Fig. 6A and B, lanes 1 and 4). Therefore, both the presence and site of termination of translation of the LP1* ORF affect the rate of synthesis of VP2 relative to that of VP3 from the major 19S mRNA species.

The leader ORF also affects the amount of VP2 plus VP3 synthesized. To determine whether the presence of the leader ORF also affects the amount of VP2 plus VP3 synthesized from the major 19S mRNA, the amount of pulse-labeled VP2 plus VP3 present in each sample was determined (Fig. 6B) and normalized to the amount of viral 19S mRNA present in the cytoplasm of cells transfected in parallel (Fig. 6C). The presence of the leader ORF decreased synthesis of VP2 plus VP3 two- to threefold (summarized in Fig. 6A). Therefore, as with the major 16S mRNA, the presence of a leader ORF decreases synthesis of the proteins encoded downstream.

At least 40 to 60% of ribosomes scan past the LP1 initiation signal on the major 19S mRNA species. Determination of the molar ratios of the pulse-labeled, immunoprecipitated VP3-related products synthesized in cells transfected with mutant SV19S(fusion) provides an independent measurement of the leakiness of the LP1 initiation signal. At least 40 to 60% of the 40S ribosomal subunits scanned past the LP1 initiation signal and initiated at VP2 or VP3 (Fig. 6B, lane 4). These results agree well with those calculated for translation of the major 16S mRNA species.

At least 20% of ribosomes bypass the consensus initiation signal when it replaces the LP1 initiation signal in the major 16S mRNA species. To determine whether the LP1 initiation signal (GCCAUGG) is in a good sequence context for efficient initiation of translation, the mutant SV16S(fusion-ACCAUGG), which differs from SV16S(fusion) by a single-base-pair substitution (altering the sequence context of the LP1 initiation signal from GCCAUGG to the optimal initiation signal, ACCAUGG), was constructed. Determination of the molar ratio of the pulse-labeled, VP1-related proteins synthesized in cells transfected with SV16S(fusion-ACCAUGG) indicated that VP1 was synthesized fairly efficiently even when the LP1 translation initiation signal was replaced by the optimal initiation signal (i.e., 20% of 40S ribosomal subunits bypassed the optimal initiation signal and

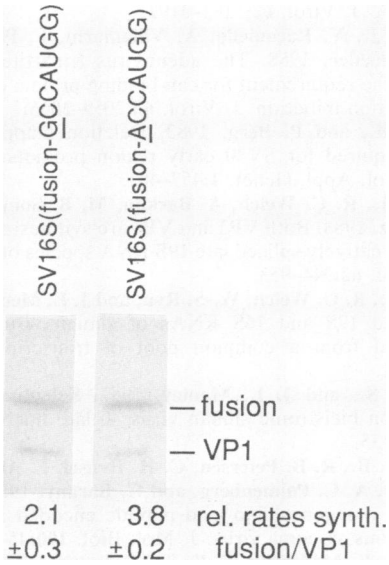

FIG. 7. Rates of synthesis of LP1-VP1 fusion relative to that of VP1 in cells transfected in parallel with the mutants SV16S(fusion-GCCAUGG) and SV16S(fusion-ACCAUGG), which differ solely in the context of the leader initiation signal. The experiment was performed essentially as described in the legend to Fig. 3. Indicated at the bottom is a summary of the data obtained from three independent experiments.

initiated at VP1 [Fig. 7]). However, 20% may be an underestimate because 40S ribosomal subunits may bypass the VP1 initiation signal and would not be measured.

DISCUSSION

Leader ORFs affect translation of downstream ORFs. The major late 16S and 19S mRNA species of SV40 each contain an ORF which begins upstream of the sequences encoding the virion proteins. To study the effects of these upstream ORFs on synthesis of the virion proteins from these mRNAs, a variety of mutants were constructed in which either the leader initiation signal was inactivated or the length and site of translation termination of the leader ORF was altered. The data obtained from the analysis of these mutants (Fig. 3, 4, and 6) show that the presence of ORFs in the leader region of mRNAs can affect both the absolute rate and, when there are two or more ORFs located downstream, the relative rates of translation of downstream ORFs. Inactivation of the LP1 initiation signal resulted in a threefold increase in VP1 synthesis from the major 16S mRNA species when the LP1 ORF did not overlap with the VP1 ORF [SV16S(−21)] and a sixfold increase when it did overlap [SV16S(fusion)] (Fig. 3). Inactivation of the LP1 initiation signal resulted in a two- to threefold increase in synthesis of VP2 plus VP3 from the major 19S mRNA species and a twofold increase in the rate of synthesis of VP2 relative to that of VP3 (Fig. 6). We reported previously that the presence of a leader ORF both reduces synthesis of VP2 and VP3 three- to fivefold from 19S mRNAs translated in a cell-free rabbit reticulocyte lysate and affects the VP2:VP3 ratio (5). These findings agree well with the in vivo results reported here. Furthermore, we show in experiments to be reported elsewhere that the SV40 leader ORF down regulates expression of a downstream ORF as much as 10-fold when its size is increased to 115 codons (J. E. Mertz, G. Gelembiuk, and J. M. Kane, manuscript in preparation). Therefore, the effects of leader ORFs on the efficiency of translation of downstream ORFs can be quite significant.

Our findings confirm that the leader ORF of SV40 decreases translation of ORFs located downstream (5, 7, 28). We showed that the presence of the LP1 initiation signal can decrease VP1 synthesis from the major 16S mRNA species threefold (Fig. 3) and VP2 plus VP3 synthesis from the major 19S mRNA species two- to threefold (Fig. 6). In contrast, Dabrowski and Alwine (2) concluded that the presence of the LP1 initiation signal does not significantly affect translation of a downstream ORF on an SV40 19S-like mRNA. A likely explanation for their finding is that a significant percentage of the SV40 late mRNA produced in their experiment lacked the LP1 initiation signal due to splicing (i.e., was analogous to RNA species A of Fig. 1) (6). If the LP1 initiation signal is not present on much of this 19S-like mRNA, inactivation of this initiation signal would be expected to have little effect.

We also showed that LP1 and VP1 are both synthesized fairly efficiently from the bicistronic 16S mRNA. In contrast, Grass and Manley (7) found that little VP1 is synthesized from a variant of the bicistronic SV40 late 16S mRNA in which the first 33 bases of the adenovirus tripartite leader are present at the 5′ end of the mRNA. Since the tripartite leader plays a role in the translation of adenovirus late mRNAs (3, 22), it may have influenced the results obtained by these workers. Another possible explanation is that the 5′ untranslated region on their variant late 16S mRNA was 73 rather than 10 bases in length, resulting in less bypassing of the LP1 initiation signal (19) (see below). On the other hand, since only a single-base substitution was introduced into the leader AUG codon in the experiments reported here, our results should be an accurate measure of how translation of the leader ORFs affects translation of the ORFs located downstream on the SV40 late mRNAs.

The effects of leader ORFs observed here may be the result of (i) efficient reinitiation of translation occurring only when the leader ORF does not overlap with the downstream ORF, (ii) translation of the leader ORF inhibiting translation of the downstream ORFs by occluding scanning to (1) or translation initiation at (14) the downstream AUGs, or (iii) some combination of the above. Although additional experiments are needed to distinguish definitively among these possible mechanisms, the data summarized in Fig. 3A indicate that at least part of the effect is due to some type of occlusion based on the following argument: whereas 3 units (U) of VP1 were synthesized when the VP1 initiation signal was the 5′ proximal AUG on the mRNA [determined from SV16S(AUG$^-$)], 1 U of protein initiating at the LP1 AUG was synthesized when the LP1 ORF was the 5′-proximal AUG on the mRNA [determined from SV16S(fusion)]. If one assumes that ribosomes loaded at equal rates onto these mRNAs, then the observation that threefold more ribosomes initiated at the VP1 initiation signal on the SV16S(AUG$^-$) mRNA than at the LP1 initiation signal indicates that two-thirds of the 40S ribosomal subunits bypassed the LP1 initiation signal. One would therefore expect 2 U (i.e., 3 U minus 1 U initiating at LP1) of VP1 synthesis from the fusion mRNA. However, only 0.5 U of VP1 was synthesized from the fusion mRNA. Synthesis of VP1 was inhibited on the WT mRNA by occlusion as well, since one would have expected 2 U of synthesis of VP1 (even without reinitiation), yet only 1 U was made (Fig. 3A).

In summary, the data presented here indicate that the frequency of bypassing the LP1 initiation signal is quite high, with much if not all of the synthesis of VP1 from the major

16S mRNA of SV40 occurring via a leaky scanning mechanism. However, the possibility that some synthesis of VP1, VP2, and VP3 occurs by a reinitiation mechanism has not been excluded.

Effect of 5′ UTR length on the efficiency of leaky scanning. Why do scanning ribosomes bypass the LP1 initiation signal at a high frequency? Kozak has hypothesized that ribosomes are unable to recognize efficiently translation initiation signals located very close to the 5′ end of an mRNA (19). Since 40S ribosomal subunits protect approximately 60 bases of RNA from nucleases (20 and references therein) and the LP1 AUG is only 10 bases from the 5′ end of the major 16S mRNA species, it is plausible that 40S ribosomal subunits bind at or near the cap and frequently begin scanning downstream of the LP1 initiation signal (19). One way to test this hypothesis is to vary systematically the distance between the 5′ end of the mRNA and the first initiation signal and then measure the amount of protein synthesized from each mRNA. Data from such an experiment indicate that 70% less VP1 is synthesized in vivo from the major late 16S mRNA when the distance between the cap and leader initiation signal is increased from 6 to 44 bases (S. A. Sedman, G. Gelembiuk, and J. E. Mertz, submitted for publication). This finding provides direct support for the hypothesis that 40S ribosomal subunits frequently bypass AUG codons located very close to the 5′ end of mRNAs. It also provides an explanation for why even the optimal translation initiation signal was quite leaky in our experiments (Fig. 7).

In summary, the results reported here and by others (5, 7, 11, 14, 23, 25, 28, 33) show clearly that the rates of synthesis of some proteins can be modulated in part by translation of ORFs encoded within the leader regions of mRNAs. In this communication we showed that leader ORFs can affect not only the overall rates of translation of downstream ORFs but also their relative rates of translation. In addition, we presented the first direct evidence that a good initiation signal can be very leaky when located close to the 5′ end of an mRNA. We also showed that LP1 and VP1 are synthesized from the WT bicistronic 16S mRNA species at approximately equal molar ratios. In addition, VP1 is synthesized predominantly via a leaky-scanning mechanism rather than by reinitiation. Finally, we showed that approximately half of the VP1 synthesized in SV40-infected cells is made from the minor, monocistronic 16S mRNA species even though it represents only 20% of the 16S mRNA present. Therefore, minor mRNA species can be physiologically significant.

ACKNOWLEDGMENTS

We thank Jim Resnick for pSV*pm*1493; Greg Gelembiuk, Renée Welch, and Bob Wisecup for excellent technical assistance; and Joyce Knutson, Bill Sugden, Howard Temin, and members of our laboratory for helpful comments on the manuscript.

This research was supported by Public Health Service grants CA-07175 and CA-22443 from the National Institutes of Health. The synthetic oligonucleotides were obtained from the DNA synthesis facility of the University of Wisconsin Biotechnology Center. P.J.G. and S.A.S. were supported in part by Public Health Service grant CA-09135 from the National Institutes of Health.

LITERATURE CITED

1. **Barkan, A., and J. E. Mertz.** 1984. The number of ribosomes on simian virus 40 late 16S mRNA is determined in part by the nucleotide sequence of its leader. Mol. Cell. Biol. **4**:813–816.
2. **Dabrowski, C., and J. C. Alwine.** 1988. Translational control of synthesis of simian virus 40 late proteins from polycistronic 19S late mRNA. J. Virol. **62**:3182–3192.
3. **Dolph, P. J., V. Racaniello, A. Villamarin, F. Palladino, and R. J. Schnieder.** 1988. The adenovirus tripartite leader may eliminate the requirement for cap-binding protein complex during translation initiation. J. Virol. **62**:2059–2066.
4. **Fromm, M., and P. Berg.** 1982. Deletion mapping of DNA regions required for SV40 early region promoter function in vivo. J. Mol. Appl. Genet. **1**:457–481.
5. **Good, P. J., R. C. Welch, A. Barkan, M. B. Somasekhar, and J. E. Mertz.** 1988. Both VP2 and VP3 are synthesized from each of the alternatively spliced late 19S RNA species of simian virus 40. J. Virol. **62**:944–953.
6. **Good, P. J., R. C. Welch, W.-S. Ryu, and J. E. Mertz.** 1988. The late spliced 19S and 16S RNAs of simian virus 40 can be synthesized from a common pool of transcripts. J. Virol. **62**:563–571.
7. **Grass, D. S., and J. L. Manley.** 1987. Selective translation initiation on bicistronic simian virus 40 late mRNA. J. Virol. **61**:2331–2335.
8. **Hackett, P. B., R. B. Petersen, C. H. Hensel, F. Albericio, S. I. Gunderson, A. C. Palmenberg, and G. Barany.** 1986. Synthesis in vitro of a seven amino acid peptide encoded in the leader RNA of Rous sarcoma virus. J. Mol. Biol. **190**:45–57.
9. **Hughes, S., K. Mellstrom, E. Kosik, F. Tamanoi, and J. Brugge.** 1984. Mutation of a termination codon affects *src* initiation. Mol. Cell. Biol. **4**:1738–1746.
10. **Jang, S. K., H.-G. Krausslich, M. J. H. Nicklin, G. M. Duke, A. C. Palmenberg, and E. Wimmer.** 1988. A segment of the 5′ nontranslated region of encephalomyocarditis virus RNA directs internal entry of ribosomes during in vitro translation. J. Virol. **62**:2636–2643.
11. **Johansen, H., D. Schumperli, and M. Rosenberg.** 1984. Affecting gene expression by altering the length and sequence of the 5′ leader. Proc. Natl. Acad. Sci. USA **81**:7698–7702.
12. **Kozak, M.** 1981. Mechanism of mRNA recognition by eukaryotic ribosomes during initiation of protein synthesis. Curr. Top. Microbiol. Immunol. **93**:81–123.
13. **Kozak, M.** 1984. Compilation and analysis of sequences upstream from the translational start site in eukaryotic mRNAs. Nucleic Acids Res. **12**:857–872.
14. **Kozak, M.** 1984. Selection of initiation sites by eucaryotic ribosomes: effect of inserting AUG triplets upstream from the coding sequence for preproinsulin. Nucleic Acids Res. **12**: 3873–3893.
15. **Kozak, M.** 1986. Point mutations define a sequence flanking the AUG initiator codon that modulates translation by eukaryotic ribosomes. Cell **44**:283–292.
16. **Kozak, M.** 1986. Regulation of protein synthesis in virus-infected animal cells. Adv. Virus Res. **31**:229–292.
17. **Kozak, M.** 1986. Bifunctional messenger RNAs in eukaryotes. Cell **47**:481–483.
18. **Kozak, M.** 1987. Effects of intercistronic length on the efficiency of reinitiation by eucaryotic ribosomes. Mol. Cell. Biol. **7**: 3438–3445.
19. **Kozak, M.** 1987. An analysis of 5′-noncoding sequences from 699 vertebrate messenger RNAs. Nucleic Acids Res. **15**:8125–8148.
20. **Kozak, M., and A. J. Shatkin.** 1978. Migration of 40 S ribosomal subunits on messenger RNA in the presence of edeine. J. Biol. Chem. **253**:6568–6577.
21. **Liu, C.-C., C. C. Simonsen, and A. D. Levinson.** 1984. Initiation of translation at internal AUG codons in mammalian cells. Nature (London) **309**:82–85.
22. **Logan, J., and T. Shenk.** 1984. Adenovirus tripartite leader sequence enhances translation of mRNAs late after infection. Proc. Natl. Acad. Sci. USA **81**:3655–3659.
23. **Marth, J. D., R. W. Overell, K. E. Meier, E. G. Krebs, and R. M. Perlmutter.** 1988. Translational activation of the *lck* proto-oncogene. Nature (London) **332**:171–173.
24. **Mertz, J. E., and P. Berg.** 1974. Defective simian virus 40 genomes: isolation and growth of individual clones. Virology **62**:112–124.
25. **Mueller, P. P., and A. G. Hinnebusch.** 1986. Multiple upstream

AUG codons mediate translational control of *GCN4*. Cell **45:** 201–207.
26. **Peabody, D. S., and P. Berg.** 1986. Termination-reinitiation occurs in the translation of mammalian cell mRNAs. Mol. Cell. Biol. **6:**2695–2703.
27. **Pelletier, J., and N. Sonenberg.** 1988. Internal initiation of translation of eukaryotic mRNA directed by a sequence derived from poliovirus RNA. Nature (London) **334:**320–325.
28. **Perez, L., J. W. Wills, and E. Hunter.** 1987. Expression of the Rous sarcoma virus *env* gene from a simian virus 40 late-region replacement vector: effects of upstream initiation codons. J. Virol. **61:**1276–1281.
29. **Resnick, J., and T. Shenk.** 1986. Simian virus 40 agnoprotein facilitates normal nuclear location of the major capsid polypeptide and cell-to-cell spread of virus. J. Virol. **60:**1098–1106.
30. **Sedman, S. A., and J. E. Mertz.** 1988. Mechanisms of synthesis of virion proteins from the functionally bigenic late mRNAs of simian virus 40. J. Virol. **62:**954–961.
31. **Tooze, J. (ed.)** 1981. DNA tumor viruses. The molecular biology of tumor viruses, part 2, 2nd ed. Cold Spring Harbor Laboratory, Cold Spring Harbor, N.Y.
32. **Wang, F., L. Petti, D. Braun, S. Seung, and E. Kieff.** 1987. A bicistronic Epstein-Barr virus mRNA encodes two nuclear proteins in latently infected, growth-transformed lymphocytes. J. Virol. **61:**945–954.
33. **Werner, M., A. Feller, F. Messenguy, and A. Pierard.** 1987. The leader peptide of yeast gene *CPA1* is essential for the translational repression of its expression. Cell **49:**805–813.